# Controlling the photoluminescence spectra of porous nc-Si–SiO$_x$ structures by vapor treatment

**V.A. Dan'ko, V.Ya. Bratus', I.Z. Indutnyi, I.P. Lisovskyy, S.O. Zlobin, K.V. Michailovska, P.E. Shepeliavyi**
*V. Lashkaryov Institute of Semiconductor Physics, NAS of Ukraine,*
*41, prospect Nauky, 03028 Kyiv, Ukraine, e-mail: indutnyy@isp.kiev.ua*

**Abstract.** The effect of HF and H$_2$O$_2$ vapor treatment on the spectral composition and intensity of photoluminescence (PL) in porous oblique deposited nc-Si–SiO$_x$ structures have been studied using FTIR, electron-spin resonance (EPR) and PL measurements. As a result of HF vapor treatment, considerable PL intensity growth and blueshift of PL peak position are observed. It is suggested that the evolution of the PL spectra in HF vapor-treated samples can be attributed to selective-etching-induced decrease in Si nanoparticle dimensions and to passivation of Si dangling bonds (that are nonradiative recombination trap states) by hydrogen and oxygen. Additional treatment in H$_2$O$_2$ vapor results in additional nc-Si surface oxidation and reduction of nc-Si size. The possibility to control the PL characteristics (peak position and intensity) of the porous nc-Si–SiO$_x$ structures in a wide range by above treatments is shown..

**Keywords:** nanocrystal, silicon oxide, photoluminescence, thin film.

## 1. Introduction

Thin-film structures containing Si nanoclusters (nc-Si) embedded into SiO$_x$ matrix attract attention of many researchers, because of their promising applications in advanced electronic and optoelectronic devices [1-5]. The structure of Si nanoparticles depends on the formation temperature: annealing at temperatures below 900 °C results in formation of amorphous inclusions, whereas at higher temperatures, the Si nanocrystals are formed.

The photoluminescence (PL) emission in such systems consists of an intense and wide emission peaking in the near-infrared or visible spectrum. With decreasing dimensions of nc-Si, the peak of the emission spectrum shifts to shorter wavelengths. The mechanism of PL in these structures is still in doubt. Some authors assume that the blueshift of the PL spectrum is mainly caused by quantum confinement of excitons in crystalline nc-Si, quantum confinement of carriers and the short carrier lifetime in the band-tail states for amorphous nc-Si [6]. Other authors consider PL as originating from the electronic states localized at defects nearby the interface between the nanoparticle and host matrix [7-8].

The most important factors influencing the characteristics of PL are nanoparticle size and state of the nanoparticle–SiO$_x$ interface. The control of nc-Si size and passivation of nonradiative states and defects at this interface is an essential requirement in order to increase the intensity of PL. The Si–SiO$_x$ interface can be modified by chemical compounds of necessary composition. Such treating is a most efficient in porous structures and at enhanced pressure and temperature [9].

Recently [10, 11], we have proposed the method of porous nc-Si–SiO$_x$ light-emitting structure formation using oblique deposition of Si monoxide (SiO) in vacuum. The electron microscopy studies show that, during this deposition, SiO$_x$ films with a porous (column-like) structure are formed, with the column diameter depending on the deposition angle. During high-temperature annealing of these films, the thermally stimulated formation of Si nanoinclusions occurs in a restricted volume of the SiO$_x$ columns. This method allows high-precision control of the thickness and porosity of the films.

Because of free space (cavities) between the oxide columns, the structures is more susceptible to chemical treatments, e.g., to treatment with acetone or ammonia vapors [9], or etching in HF solution [12, 13]. Such

treatments modify the nc-Si–SiO$_x$ interface, nanoparticle size and, thus, influence the light-emission properties. But wet etching of nc-Si–SiO$_x$ porous structures results in removing some nanoparticles into solution. This causes the decreasing of PL intensity.

In this paper, we investigate the effect of chemical treatment in HF and H$_2$O$_2$ vapors on the PL and IR spectra of the porous light-emitting nc-Si–SiO$_x$ structures produced by oblique deposition in vacuum.

## 2. Experiment

Thin SiO$_x$ films were deposited onto two-side polished c-Si (111) substrates using thermal evaporation of 99.9% pure silicon monoxide SiO (Cerac Inc.) in vacuum ((1–2)×10$^{-3}$ Pa). Before deposition, the substrates were oriented at the angle of 60° between the normal to the substrate surface and direction to the evaporator. The evaporation rate was monitored *in situ* by the quartz-crystal-oscillator monitor system (KIT-1). The as-deposited film thickness was measured using MII-4 microinterferometer and amounted to 850 nm. Because of additional oxidation by residual gases during evaporation of SiO, the compositionally nonstoichiometric SiO$_x$ ($x > 1$) films were deposited in the vacuum chamber. The films were annealed in vacuum for 15 min at the temperature 975 °C. This high-temperature annealing leads to decomposition of SiO$_x$ into Si and SiO$_2$ and formation of Si nanoclusters embedded into oxide matrix [1-3].

Annealed nc-Si–SiO$_x$ samples were placed in closed cell with HF vapor flow at the temperature 30 °C. Treatment in HF vapor results in selective etching the SiO$_2$ inclusions in porous heterogeneous nc-Si–SiO$_x$ structure. Some of HF etched samples were kept for one hour in the pressure-tight autoclave that contained a certain amount of hydroxide (H$_2$O$_2$) at the temperature 150 °C, the pressure of hydroxide vapors being 37 atm.

PL spectra were measured at room temperature within the wavelength range of 440–900 nm using 337-nm line of a nitrogen laser as an excitation source. These spectra were normalized to the spectral sensitivity of the experimental system. The structure of the obliquely deposited SiO$_x$ films was studied by ZEISS EVO 50XVP high-resolution electron microscope. FTIR measurements were carried out with Perkin-Elmer Spectrum BXII spectrometer. EPR spectra were studied at room temperature by using the X-band spectrometer with 100-kHz modulation of the magnetic field.

## 3. Results and discussion

Results of SEM investigations of oblique deposited SiO$_x$ samples were shown in the previous papers [9, 12]. These films possess a porous (inclined column-like) structure with the column diameter varying within the range 10 to 100 nm. The dimensions of the columns, their orientation, and porosity (relative volume of pores) of the films depend on the angle of deposition. The porosity of samples deposited at β = 60° is equal to 34% [11]. High-temperature annealing of oblique deposited SiO$_x$ films do not change porosity and column-like structure of the samples.

The normalized PL spectra of the nc-Si–SiO$_x$ samples annealed and HF vapor treated have been shown in Fig. 1. The emission spectrum of the initial annealed but unetched sample (curve 1) exhibits a broad band, with the peak position at 820 nm in the near-infrared region. Curves 2, 3, and 4 in Fig. 1 correspond to the samples etched in the HF vapor for 1.5, 10, and 30 min, respectively. With increasing the time of etching, we observe a gradual shift of the emission peak to shorter wavelengths and increase in the PL intensity. In particular, after etching for 10 min the PL band peak position reached ~700 nm, and the PL intensity became near 200 times higher in its magnitude than that of the initial annealed sample. The further increase of the etching time for samples ($t > 10$ min) is accompanied by a further short-wavelength shift of the emission band as well as a gradual decrease in the emission intensity (Fig. 2), because of reduction both the film thickness and amount of silicon in nanoclusters.

Fig. 3 shows the normalized PL spectra for the nc-Si–SiO$_x$ samples annealed and HF vapor treated for 10 min (curve 1), and subsequently H$_2$O$_2$ vapor treated (curve 2). As in Fig. 1, HF treatment results in the blueshift of the PL peak and in huge enhancement in the PL intensity. Further treatment in H$_2$O$_2$ vapor results in a further shift of the PL peak to shorter wavelengths (to 640 nm) and a small decrease in the PL intensity (by 30%).

It should be mentioned that during HF vapor etching, the thickness of the nc-Si–SiO$_x$ samples diminishes gradually, but at H$_2$O$_2$ treatment the thickness does not change.
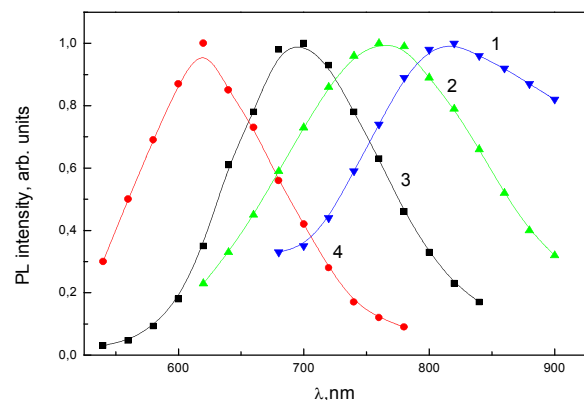


**Fig. 1.** Normalized room temperature PL spectra of the nc-Si–SiO$_x$ samples annealed at 975 °C (*1*), then HF vapor treated for 1.5 (*2*), 10 (*3*), and 30 min (*4*).
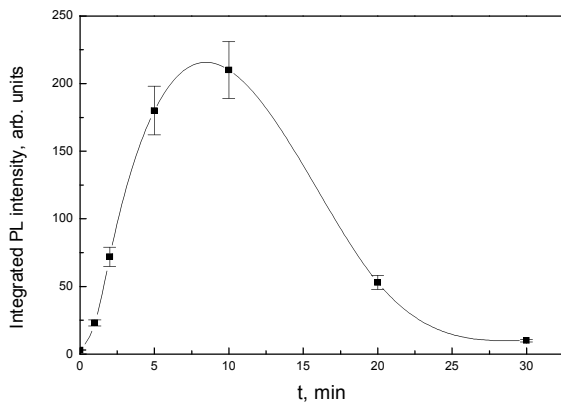
**Fig. 2.** Integrated PL intensity of the porous nc-Si–SiO$_x$ sample as a function of time of HF vapor treatment. The curve has been guided as a result of cubic-spline approximation.
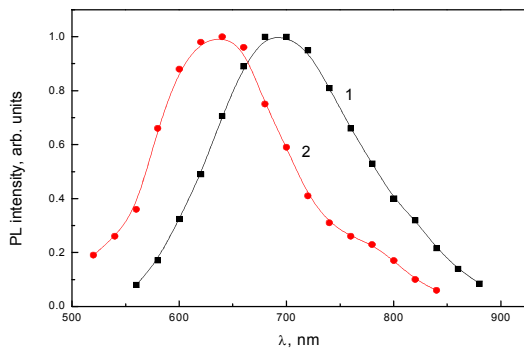


**Fig. 3.** Normalized room temperature PL spectra of the nc-Si–SiO$_x$ samples annealed and HF vapor treated for 10 min (*1*), and additionally treated with the H$_2$O$_2$ vapor (*2*).

Fig. 4 shows the FTIR spectra for the as-deposited SiO$_x$ film (curve 1), annealed (curve 2), 10 min HF-treated (curve 3) and HF and H$_2$O$_2$-treated (curve 4) samples. The absorption bands at 432, 880, and 106 cm$^{-1}$ are observed for the as-deposited sample. When the initial sample was annealed, IR peaks were shifted to 458, 810, and 1082 cm$^{-1}$. These peaks may be attributed to the vibration Si–O–Si bending mode and symmetric and asymmetric Si–O–Si stretching modes, respectively [14].

The composition of the films (parameter *x*) can be determined using compositional dependence of the position of the main IR band in spectra of SiO$_x$ layers within the range of 1000 to 1100 cm$^{-1}$, as it was ascertained in [15]. This band corresponds to the Si–O–Si stretching mode. Since the vibrations of only oxygen atoms in the silicon-oxygen phase are active in this spectral range, while the Si–Si bond vibrations cannot be recorded, this method can be used to determine the composition of the oxide matrix in as-deposited, annealed, and treated samples containing the silicon phase. The stoichiometric parameter *x,* determined by this method, is 1.73 for the as-deposited, 1.96 – for annealed, 1.8 – for 10 min HF-treated, and 1.87 – for HF and H$_2$O$_2$ – treated samples.

After HF vapor etching, the intensity of Si–O modes decreased drastically (near one order of magnitude for the annealed sample), and the peaks position were shifted (450-460, 878, and 1068 cm$^{-1}$) more close to IR peaks position for the as-deposited sample. This peak shift and decrease of the Si–O band intensity for the HF-treated sample were caused by etching the SiO$_2$ regions in porous oxide matrix.
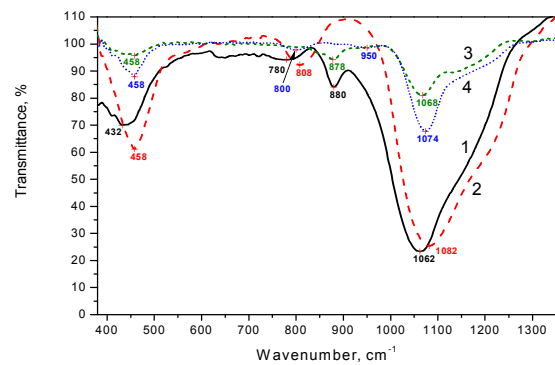


**Fig. 4.** FTIR spectra of as-evaporated (*1*), annealed at 975 °C (*2*), then HF vapor treated for 10 min (*3*), and additionally treated with the H$_2$O$_2$ vapor (*4*) nc-Si–SiO$_x$ samples.
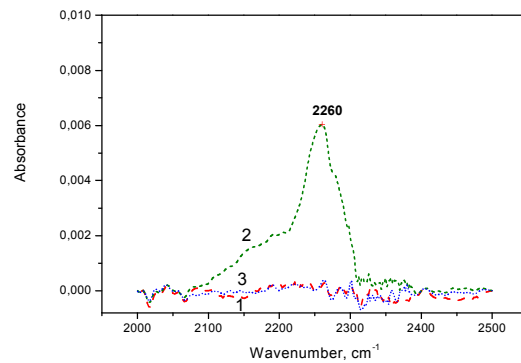


**Fig. 5.** IR absorbance of annealed at 975 °C (*1*), then HF vapor treated for 10 min (*2*), and additionally treated with the H$_2$O$_2$ vapor (*3*) nc-Si–SiO$_x$ samples.

Besides, new IR absorption peaks at ~2160 and ~2260 cm$^{-1}$ were observed in the IR spectra of HF treated samples (Fig. 5). These bands are associated with oxidized hydride (O$_2$SiH$_2$, O$_3$SiH) [14], or SiH(Si$_{3-y}$O$_y$) vibrational groups on the nc-Si surface [16].

When HF processed sample was additionally treated with $H_2O_2$, the intensity of Si–O stretching mode was approximately two times increased and main IR peak was shifted to 1074 cm$^{-1}$ ($x = 1.87$). But absorption peaks within the range 2100 to 2300 cm$^{-1}$ disappeared. These facts indicate the additional oxidation of suboxide matrix (increase of $x$) and surface of the silicon nanoparticles. In addition, the hydrogen that passivates the dangling bonds is substituted by oxygen.

Fig. 6 shows the EPR spectra of annealed samples before (curve 1) and after (curve 2) treatment in HF vapor. A nearly symmetric EPR line with a zero-crossing at g-value about 2.0049±0.0002 and peak-to-peak linewidth of 0.74 mT has been detected for obliquely deposited and annealed films. This line is attributed to dangling bonds of Si atoms in structural tetrahedra Si–Si$_3$O and, probably, in amorphous Si precipitates [2]. The bulk concentration of paramagnetic defects was close to $3.1 \times 10^{18}$ cm$^{-3}$. This result is indicative of an amorphous structure of the nc-Si inclusions in our samples, in spite of sufficiently high annealing temperature (975 °C). But, despite many works on this topic, the temperature of nc-Si crystallization in oxide matrix remains controversial. According to some authors, annealing at temperatures below 900 °C results in formation of amorphous inclusions, whereas at higher temperatures, the Si nanocrystals are formed [17-19]. Another authors concluded that silicon nanocrystals are formed at temperatures higher 1000 °C [5, 20, 21]. Probably, at this intermediate temperature (900 to 1000 °C) both amorphous and crystalline nc-Si exist in oxide matrix, or silicon nanoparticles have two-phase structure: crystalline core and amorphous surface shell.
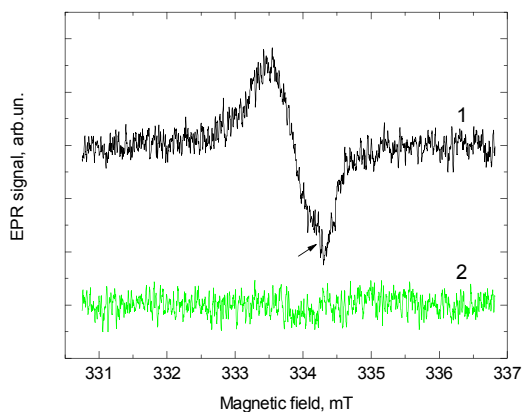


**Fig. 6.** Room temperature EPR spectra of obliquely deposited and annealed SiO$_x$ films before (*1*) and after (*2*) treatment in HF vapor, microwave frequency $\nu = 9.368$ GHz.

The weak narrow line at g = 2.0025 pointed out by an arrow in Fig. 6 can be enhanced with prolonged annealing. This EPR line has been assigned to the *EX*

center [22]. No EPR signal has been found after HF vapor treatment testifying complete passivation of dangling bonds. This result indicates that most of the Si dangling bonds existing on the nc-Si surface are effectively passivated with the hydrogen and oxygen atoms in the process of the HF treatments. Hydrogen and/or oxygen passivation on the nc-Si surface were confirmed by FTIR spectroscopy (IR absorption peaks at around 2160, and 2260 cm$^{-1}$), too.

It would be reasonable to assume that the blueshift of PL band in HF vapor-treated samples can be attributed to the selective-etching-induced decrease in the Si nanoparticle dimensions. In the porous films studied here, vapor of the etching agent penetrates deep into the entire film and dissolves SiO$_2$ at the surface of the oxide columns, thus stripping nc-Si. After HF treatment, the nc-Si newly forms a thin native oxidized layer on the surface when exposing it to atmospheric oxygen that easily penetrates via pores into the film and, first of all, forms chemical bonds with the Si atoms located in the outer layers of nc-Si. Because of oxidation of the nc-Si surface, dimensions of the initial nc-Si core are reduced, resulting in the blueshift of the emission spectrum. Additional treatment in $H_2O_2$ vapor results in additional nc-Si surface oxidation and reduction of nc-Si size.

Huge enhancement in the PL intensity of about two hundreds times during HF vapor treatment can be related to the passivation of Si dangling bonds (that are nonradiative recombination trap states) by hydrogen and oxygen.

These interpretations are consistent with the results of FTIR and EPR measurements.

## 4. Conclusions

In this study, the effect of HF and $H_2O_2$ vapor treatment on the emission spectra of the porous light-emitting nc-Si–SiO$_x$ structures is analyzed. As a result of HF vapor treatment, an increase in the PL intensity and a spectral shift of PL peaks to shorter wavelengths (maximum blueshift was more than 200 nm) are observed. Besides, during the first period of vapor treatment the intensity of PL peak increased near 200 times in its magnitude. At the further HF vapor etching, the PL intensity diminishes gradually with decreasing the film thickness.

From FTIR and EPR measurements, it has been determined that the HF vapor treatment results in selective etching of SiO$_2$ regions in porous oxide matrix, and most of the Si dangling bonds (nonradiative recombination trap states), existing on the nc-Si surface, are effectively passivated with the hydrogen and oxygen atoms. Thus, the increase in the PL intensity is caused by this passivation of nonradiative states. It is assumed that the blueshift of PL spectrum is caused by a decrease in nc-Si sizes due to etching the porous SiO$_2$ matrix in HF vapor and following oxidation of the nc-Si surface. Additional treatment in $H_2O_2$ vapor results in additional nc-Si surface oxidation and reduction of nc-Si size without etching the oxide matrix and decrease of the sample thickness.

The obtained results have shown that using HF and $H_2O_2$ vapor treatment of light-emitting porous nc-Si–$SiO_x$ structures it is possible to control PL intensity and peak position in a spectral wide range.

*References*

1.  M. Molinary, H. Rinnert and H. Vergnat, Visible photoluminescence in amorphous $SiO_x$ thin films prepared by silicon evaporation under a molecular oxygen atmosphere // *Appl. Phys. Lett.* **82**, p. 3877-3879 (2003).
2.  V.Ya. Bratus', V.A. Yukhimchuk, L.I. Berezhinskii, M.Ya. Valakh, I.P. Vorona, I.Z. Indutnyi, T.T. Petrenko, P.E. Shepelyavyi, and I.B. Yanchuk, Structural transformations and silicon nanocrystallite formation in $SiO_x$ films // *Fizika tekhnika poluprovodnikov* **35**, p. 854-859 (2001) [*Semiconductors* **35**(7), p. 821-826 (2001)].
3.  D. Nesheva, C. Raptis, A. Perakis et al., Raman scattering and photoluminescence from Si nanoparticles in annealed $SiO_x$ thin films // *J. Appl. Phys.* **92**, p. 4678-4683 (2002).
4.  J. Heitmann, F. Müller, M. Zacharias, U. Gösele, Silicon nanocrystals: size matters // *Adv. Mater.* **17**, p. 795 (2005).
5.  S. Hernández, A. Martínez, P. Pellegrino, Y. Lebour, B. Garrido, E. Jordana, and J.M. Fedeli, Silicon nanocluster crystallization in $SiO_x$ films studied by Raman scattering// *J. Appl. Phys.* **104**, 044304 (2008).
6.  Yoshihiko Kanemitsu, Efficient light emission from crystalline and amorphous silicon nanostructures // *J. Luminescence* **100**, p. 209-217(2002).
7.  M.V. Wolkin, J. Jorne, P.M. Fauchet, G. Allan, C. Delerue, Electronic state and luminescence in porous silicon quantum dots: the role of oxygen // *Phys Rev. Lett.* **82**, p. 197 (1999).
8.  M. Ippolito, S. Meloni, and L. Colombo, Interface structure and defects of silicon nanocrystals embedded into a-$SiO_2$ // *Appl. Phys. Lett.* **93**, 153109 (2008).
9.  I.Z. Indutnyi, K.V. Michailovska, V.I. Min'ko, P.E. Shepeliavyi, Effect of acetone vapor treatment on photoluminescence of porous nc-Si–$SiO_x$ nanostructures // *Semiconductor Physics, Quantum Electronics & Optoelectronics* **12**(2), p. 105-109(2009).
10. I.Z. Indutnyy, I.Yu. Maidanchuk, V.I. Min'ko, Visible photoluminescence from annealed porous $SiO_x$ films // *J. Optoelectron. and Adv. Mater.* **7**, p. 1231-1236 (2005).
11. V.A. Dan'ko, I.Z. Indutnyy, I.Y. Maidanchuk, V.I. Min'ko, P.E. Shepelyavyi, and V.A. Yukhimchuk, Formation of the photoluminescence structure based on $SiO_x$ porous films // *Optoelektronika i poluprovodnikovaya tekhnika* **39**, p. 65-72 (2004), in Ukrainian.
12. I.Z. Indutnyi, E.V. Michailovskaya, P.E. Shepeliavyi, and V.A. Dan'ko, Visible photoluminescence of selectively etched porous nc-Si–$SiO_x$ structures // *Fizika tekhnika poluprovodnikov* **44**(2), p. 218-222 (2010) [*Semiconductors* **44**(2), p. 206-210 (2010)].
13. Keisuke Sato and Kenji Hirakuri, Improved luminescence intensity and stability of nanocrystalline silicon due to the passivation of nonluminescent states // *J. Appl. Phys.* **97**, 104326 (2005).
14. R.W. Liptak, U. Kortshagen, and S.A. Campbell, Surface chemistry dependence of native oxidation formation on silicon nanocrystals // *J. Appl. Phys.* **106**, 064313 (2009).
15. M. Nakamura, Y. Mochizuki, K. Usami et al., Infrared absorption spectra and compositions of evaporated silicon oxide ($SiO_x$) // *Solid State Communs.* **50**, p. 1079-1081 (1984).
16. Ikurou Umezu, Akira Sugimura, Toshiharu Makino, Mitsuru Inada, and Kimihisa Matsumoto, Oxidation processes of surface hydrogenated silicon nanocrystallites prepared by pulsed laser ablation and their effects on the photoluminescence wavelength // *J. Appl. Phys.* **103**, 024305 (2008).
17. B.J. Hinds, F. Wang, D.M. Wolfe, C.L. Hinkle, and G. Lucovsky, Investigation of post-oxidation thermal treatments of Si/$SiO_2$ interface in relationship to the kinetics of amorphous Si suboxide decomposition // *J. Vac. Sci. Technol. B* **16**(4), p. 2171-2176 (1998).
18. Keisuke Sato, Naoki Kishimoto, Kenji Hirakuri, White luminescence from silica glass containing red/green/blue luminescent nanocrystalline silicon particles // *J. Appl. Phys.* **102**, 104305 (2007).
19. Wei Pan, R.G. Dunn, M.S. Carroll, J.C. Banks, L.N. Brewer, Photoluminescence in silicon rich oxide thin films under different thermal treatments // *J. Non-Crystalline Solids* **354**, p. 975-977(2008).
20. N. Daldosso, G. Das, S. Larcheri, G. Mariotto, G. Dalba, L. Pavesi, A. Irrera, F. Priolo, F. Iacona, F. Rocca, Silicon nanocrystal formation in annealed silicon-rich silicon oxide films prepared by plasma enhanced chemical vapor deposition // *J. Appl. Phys.* **101**, 113510 (2007).
21. I. Stenger, B. Gallas, L. Siozade, C.-C. Kao, S. Chenot, S. Fisson, G. Vuye, and J. Rivory, Evolution of the optical properties of Si nanoparticles embedded in $SiO_2$ as function of annealing conditions // *J. Appl. Phys.* **103**, 114303 (2008).
22. A. Stesmans New intrinsic defect in as-grown thermal $SiO_2$ on (111)Si // *Phys. Rev.* **B 45**(16), p. 9501-9504 (1992).